Journal of Hydrology 524 (2015) 15–29

Contents lists available at ScienceDirect

Journal of Hydrology

journal homepage: www.elsevier.com/locate/jhydrol

Groundwater dynamics and surface water–groundwater interactions in a prograding delta island, Louisiana, USA

Michael T. O'Connor [a,*], Kevan B. Moffett [a,b]

[a] Department of Geological Sciences, The University of Texas at Austin, Austin, TX, United States
[b] School of the Environment, Washington State University Vancouver, Vancouver, WA, United States

ARTICLE INFO

Article history:
Received 18 July 2014
Received in revised form 6 February 2015
Accepted 7 February 2015
Available online 17 February 2015
This manuscript was handled by Konstantine P. Georgakakos, Editor-in-Chief, with the assistance of Marco Toffolon, Associate Editor

Keywords:
Delta islands
Hydrology
Groundwater dynamics
Coastal deltas
Cold fronts

SUMMARY

Deltas in coastal environments are assumed to function as chemical "buffers", filtering nutrient-rich terrestrial runoff through the island structures and aquatic ecosystems as it travels to the sea, but the magnitude of this effect cannot be accurately quantified without understanding the physical relationships between the surface water and groundwater. The groundwater hydrology of young, prograding delta systems and its relationship to surrounding surface water dynamics are poorly understood.

This study developed a new conceptual model of the hydrology of a prograding delta island groundwater system. The study was based on field data collected at Pintail Island, a 2 km^2 island within the Wax Lake Delta in Louisiana. Hydraulic properties and processes were quantified at multiple depths and locations spanning the island elevation gradient. Groundwater and surface water levels were monitored. A weather station recorded precipitation, air, and wind conditions.

The groundwater within Pintail Island was both spatially and temporally dynamic throughout the study period of 9-September-2013 to 4-February-2014. The aquifer within the distal limbs of the island responded to surface water dynamics as a connected, saturated unconfined aquifer would, and its groundwater was controlled by the surrounding surface water fluctuations of semi-diurnal winds and tides. The aquifer within the older, higher elevation island apex was a lower-permeability system with subaerial fine sediments overlying deeper, sandier sediments. In contrast to the more bayward zone of the island, this more interior zone was controlled by storm recharge, low-permeability sediments, and low head gradients, but little affected by diurnal surface water fluctuations. Groundwater flow was directed outward from the interior of the island apex and the levees toward the delta channels and the central island lagoon, but storms and high tides temporarily reversed flow directions at some locations and times, likely with significant biogeochemical consequences. This empirically-based conceptual model of the heterogeneous and dynamic hydrogeology of a young, prograding delta island provides an essential foundation for further study of prograding coastal delta island hydrology, ecology, and nutrient exchange.

1. Introduction

The geomorphology of a river delta dictates its eventual sedimentology and hydrogeologic properties (Li et al., 2009), yet the groundwater dynamics of young delta islands and their interactions with co-evolving surface water dynamics and sediment deposition remain open questions. Young deltas often develop distinct island-channel patterns (Gumbricht et al., 2004; Wellner et al., 2005), with the specific mechanisms for how these patterns develop the subject of much active research (Slingerland and Smith, 2004; Parker and Sequeiros, 2006; Kim et al., 2009; Shaw et al., 2013). Delta systems tend to be aerially extensive and low-relief, so small fluctuations in surface water level can substantially alter the amount of exposed land (Branhoff, 2012; Hiatt et al., 2014; Smith, 2014) and surface water–groundwater interface area. Over long timescales, sediment deposition in deltas is dominated by regional cycles; however, over short timescales, variations in surface water velocities during depositional events lead to well-sorted deposits (Roberts, 1997), often resulting in a general trend of increasing grain size with depth on delta islands (Nichols, 2013).

These morphological properties of prograding coastal deltas have hydrologic and hydrogeologic implications. The low relief of a delta, combined with river and/or tidal stage changes, could induce frequently varying surface water/groundwater exchange,

* Corresponding author. Tel.: +1 (631) 357 2522.
E-mail address: mtoconnor12@gmail.com (M.T. O'Connor).

http://dx.doi.org/10.1016/j.jhydrol.2015.02.017
0022-1694/

which would influence groundwater flow paths (Harvey et al., 1987; Bardini et al., 2012), further modified by sediment structure. For example, a study in a South Carolina salt marsh showed that a lower-permeability sediment layer at the surface of a marsh decreased the vertical connectivity between the surface and shallow subsurface such that the dominant hydrogeologic forcings were lateral (Wilson et al., 2011). Additionally, it has been shown that mature delta systems can play a significant role in transmitting river water to oceans through channels with sandy in-fill, as they become preferential conduits for groundwater flow and submarine discharge (Kolker et al., 2013). Changing groundwater conditions will also influence system biogeochemistry, as the amounts of available oxygen, dissolved organic carbon, and nutrients in the subsurface change with inundation (Postma et al., 1991; Bardini et al., 2012; Gonneea et al., 2013). Over large land areas, these biogeochemical processes could greatly influence the resultant water chemistry of the system, as has been shown, for example, for the Mississippi River delta system (Bianchi et al., 2013).

As delta islands compose the majority of surface area within young prograding deltas (Gumbricht et al., 2004; Wellner et al., 2005), understanding the shallow groundwater dynamics within these islands and their interactions with the surrounding channels is a critical component of a comprehensive understanding of deltas on the whole. These dynamics remain poorly understood. A number of near-analogues have been studied with respect to their hydrogeology, however, and these studies provide insight on how shallow groundwater might behave in coastal delta islands.

Ancient deltas might be thought of as helpful analogues for young (Holocene-aged) prograding coastal deltas, but they are fundamentally hydrogeologically different. The hydrogeology of old inland deltas, such as the Okavango Delta in Botswana, and old coastal deltas, such as the Nile Delta in Egypt and the Ganges/Brahmaputra Delta in India and Bangladesh, have been investigated, e.g., for reasons related to modern anthropogenic groundwater contamination and subsidence. These systems, having undergone deposition over much longer time periods, are the result of numerous deltaic lobes, each with channels and islands that have been continually filled in over time (Stanley, 1990; Alam, 1996; McCarthy, 2006). This sedimentological heterogeneity causes complex hydrogeological heterogeneity. For example, investigation of the Mississippi River Delta has shown that, although the system is relatively uniform overall, filled-in paleochannels provide heterogeneity and allow for preferential groundwater flow and submarine discharge through deep aquifer layers (Kolker et al., 2013). In contrast, young coastal delta islands are expected to be smaller, stratigraphically shallow, and less hydrogeologically complex as there has not yet been much channel avulsion/in-filling. The groundwater of mature or inland delta systems is also not as strongly dominated by the contemporary coastal dynamics, e.g., tides and onshore/offshore winds, that have been shown to be a significant driver of surface water fluctuations in young coastal deltas (Allison et al., 2000; Habib and Meselhe, 2006; Snedden et al., 2007; Geleynse et al., 2014; Hiatt et al., 2014).

Fluvial island bars and barrier islands are near-analogues for the hydrogeology of young delta islands. Like coastal delta islands, these systems are strongly influenced by surface water conditions. Fluctuations in surrounding surface water level by tides, river stage, or both lead to different zones of inundation within a fluvial or barrier island (Anschutz et al., 2009; Cardenas, 2010; Cardenas and Jiang, 2011; Bardini et al., 2012). These islands have been identified as potential hot-spots for nutrient processing due to the resulting dynamic redox conditions (Anschutz et al., 2009). In barrier islands, the consistent ocean wave action provides the potential for rapid surface water/groundwater exchange at the island margins and causes lateral groundwater pulses that dissipate inland (Li and Barry, 2000; Horn, 2002). Coastal delta islands have the potential to exhibit lateral pressure responses similar to barrier islands and nutrient processing similar to freshwater fluvial islands. However, fluvial and barrier islands differ from coastal delta islands in their sedimentology, tending to be of more poorly sorted and coarse grain sizes (Nichols, 2013). Additionally, barrier islands are surrounded by saline water, which influences the groundwater geochemistry and island ecology (Reide Corbett et al., 2000; Anderson and Evans, 2002; Röper et al., 2012). Rapidly prograding coastal deltas are instead generally dominated by large, sustained freshwater continental discharge volumes (Shaw et al., 2013).

Unlike the differing sedimentology of fluvial/barrier and delta islands, the sedimentology of coastal salt marshes and delta islands can be similar. Like many delta islands, salt marshes can often be described as fining upwards, with coarser sediments overlain by fine organic matter and mud (Hughes et al., 1998; Wilson et al., 2011). Studies of salt marsh hydrology have shown that the hydraulic conductivity of the sediment directly influences groundwater flow paths and surface water/groundwater interactions (Hughes et al., 1998; Wilson et al., 2011; Moffett et al., 2012) and that low conductivity sediments in a region of significant plant transpiration can cause unsaturated 'pockets' within the otherwise saturated sediments (Ursino et al., 2004; Zhang et al., 2013, p.201; Boaga et al., 2014). Tidal cycling occurring on longer timescales (e.g., spring/neap, seasonal) also provides potential for long term surface water–groundwater exchange (Lenkopane et al., 2009). Similar effects might be expected in a coastal delta, although without the influence of high salinity.

The ecosystem services provided by a coastal delta distinguish it from its near-analogues. Coastal deltas receive large volumes of continental runoff, often with high concentrations of nitrate and phosphate from agriculture (Goolsby et al., 2000). The coastal delta provides a final opportunity for these nutrients to be consumed through microbial metabolism in benthic, hyporheic, and bank sediments, and slow-flowing wetland water columns, prior to discharge to the sea (Spalding and Parrott, 1994; Musslewhite et al., 2003; Rivera-Monroy et al., 2010). Some land management policies now consider the potential for these processes to occur on a large scale: for example, the Louisiana Coastal Master Plan of 2012 cites the development of new coastal wetland area as a potential remedy to the growing anoxic zone in the Gulf of Mexico (Rabalais et al., 1996; Peyronnin et al., 2013). The nutrient-buffering capacity of coastal wetland and delta systems continues to be an active area of research (Venterink et al., 2003; Rivera-Monroy et al., 2010; Henry, 2012) yet there is, so far, little research attempting to connect the nutrient buffering capacity of young prograding coastal deltas with their groundwater hydrology. An accurate understanding of delta groundwater dynamics is prerequisite to developing realistic and comprehensive biogeochemical reaction estimates.

This study provided a first empirical inspection of shallow groundwater flow patterns within a young, newly prograding delta island of the Wax Lake Delta of coastal Louisiana. Time series of groundwater and surface water hydraulic potentials within and around the island were analyzed and compared to environmental forcing factors such as onshore/offshore winds, tides, river discharge, and rain events. Existing sediment data were combined with new observations to characterize the hydrogeologic structure and flow systems within the island and to identify their influence from the surface water. Groundwater dynamics were analyzed with respect to spatial location within the island (and so within its heterogeneous sedimentology), as well as with respect to differences in temporal responses to environmental forcing factors. Based on the field evidence, we developed a conceptual model for young, prograding delta island hydrogeology and the key factors in its spatio-temporal dynamics, which may now be tested at other locations.

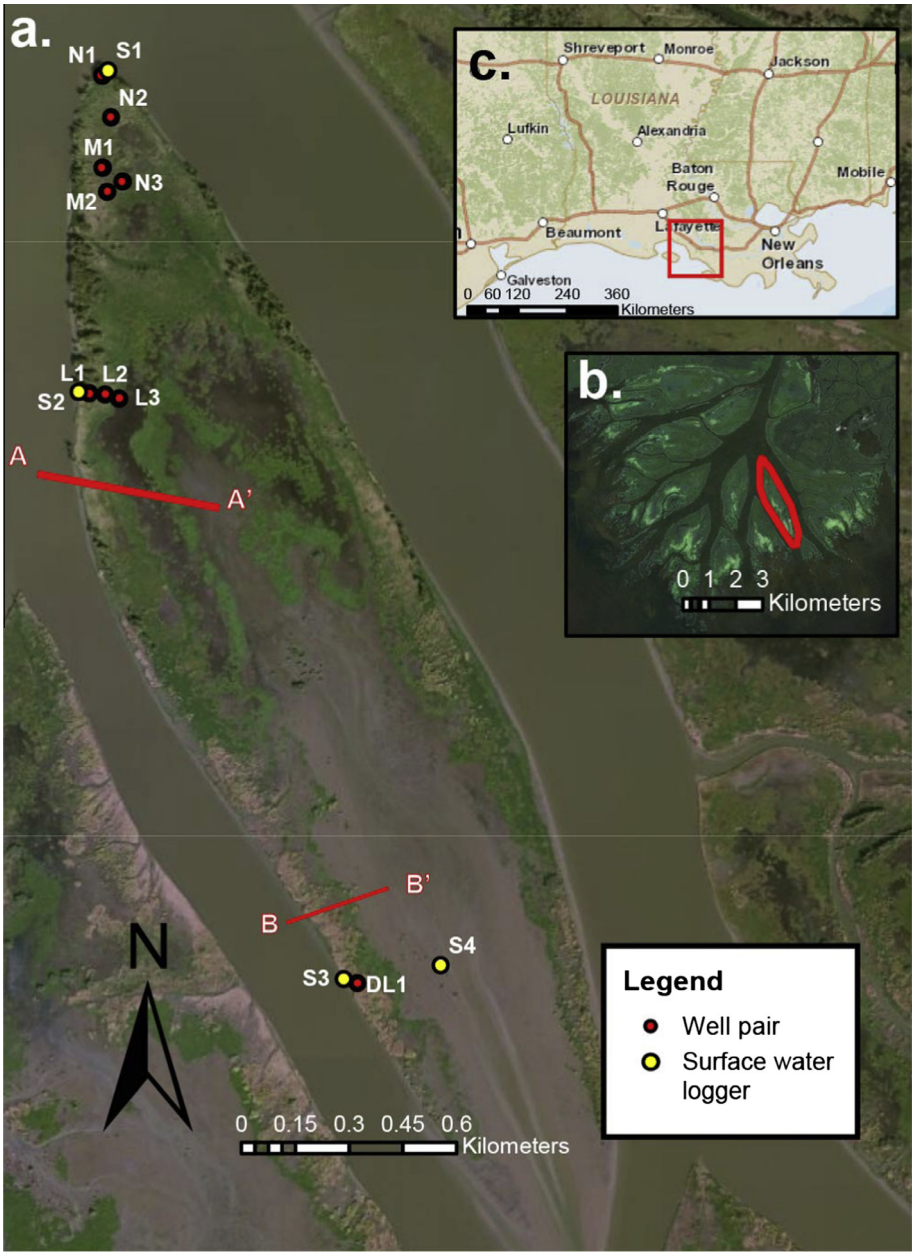

Fig. 1. (a) Map of Pintail Island and measurement locations. Cross-sections A–A′ and B–B′ correspond to schematic cross-sections in Fig. 2. (b) Location of Pintail Island within Wax Lake Delta and (c) within Louisiana. Background imagery from ESRI.

2. Study site and methods

2.1. Study site

The Wax Lake Delta (29.5226° N, 91.4367° W) is a roughly 100 km^2, rapidly prograding delta 130 km southwest of New Orleans, Louisiana. It is characterized by large, chevron-shaped islands and narrow channels. It is supplied by the Wax Lake Outlet, a man-made channel excavated in 1941 by the US Army Corps of Engineers (Roberts, 1997). The Wax Lake Outlet is fed by the Atchafalaya River and receives roughly 10% of the total water flow of the Mississippi River system (Parker and Sequeiros, 2006). Although the delta protrudes into Atchafalaya Bay, salinity measurements are very low for many kilometers beyond the delta shoreline, making it a freshwater-dominated system (Shaw et al., 2013). Atchafalaya Bay is a shallow platform, with an average depth of roughly 2 m (Neill and Allison, 2005). The Wax Lake Delta developed subaqueously into the bay from 1941 until 1973; in 1973, a large flood delivered enough sediment to the system that it became subaerial (Wellner et al., 2005).

This study focused on Pintail Island, one of the older islands in the delta (Fig. 1). Pintail Island is a roughly 2 km^2 island, 0.7 km wide at its widest point and 3.2 km long along its major axis. The relief of the island is roughly 50 cm from the highest to lowest subaerial points (Lidar survey, National Center for Airborne Laser Mapping, 2009). The island vegetation zonation follows its elevation profile, with the highest elevations dominated by *Salix nigra* (black willow), slightly lower elevations by *Colocasia esculenta* (elephant ear), the often-flooded inner island by *Nelumbo lutea* (lotus) and various reed species, and the lowest elevations constituting an aquatic lagoon within the central island (Viparelli et al., 2011; Carle et al., 2013) (Fig. 2). The highest-elevation parts of Pintail Island are along the levees nearest to its apex (north), and the lowest-elevation parts are more distal, farthest toward the bay (south).

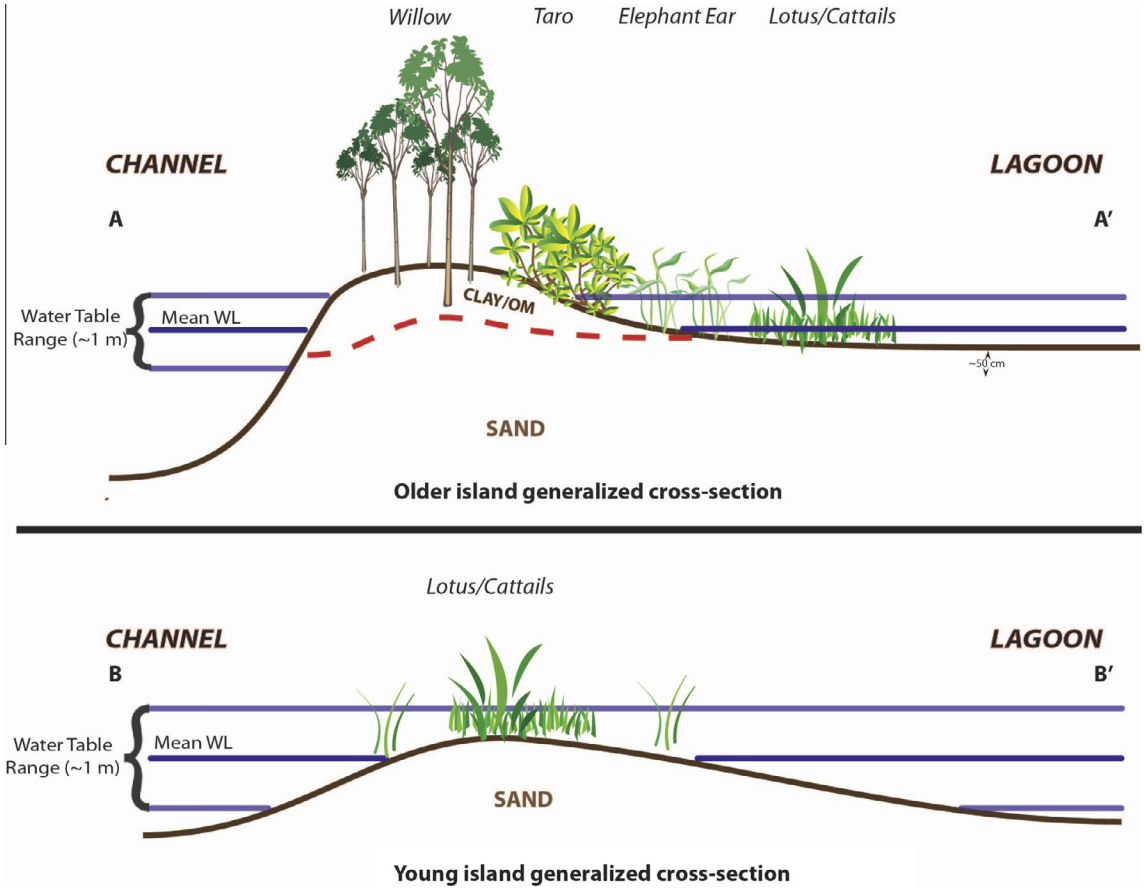

Fig. 2. Schematic island cross sections with schematic sediment properties and vegetation. Locations A–A′ and B–B′ as approximated in Fig. 1.

Prior studies of the surface water dynamics of Wax Lake Delta documented a 20–30 cm microtide (Shaw et al., 2013) and an often more substantial surface water influence by onshore and offshore winds (Geleynse et al., 2014). These tide and wind influences were also confirmed for the central lagoon of Pintail Island, which detains a significant amount of surface water flow from the channels (Hiatt et al., 2014).

This study made use of tidal predictions for Point Cheveruil, LA (10.6 km west of the Pintail Island apex (NOAA, 2014) and discharge data for the Atchafalaya River at Simmesport, LA (USGS Station 07381490 (USGS, 2014)). Although a USGS gage station existed closer to the field site in Calumet, data inspection showed that station was apparently influenced by a tidal or diurnal cycle that distorted the representation of river discharge and therefore made its records unsuitable as an independent variable representing continental runoff. Correlation verified that the discharge at Simmesport was linearly proportional to discharge at Calumet over daily and longer timescales, supporting the use of the Simmesport gage data as the relevant, independent "discharge" variable for this study's purposes. Also, the linear analyses of this study were based on changes in discharge, rather then absolute discharge values, so gages with proportional discharges would yield mathematically proportional results. Additional details on these gages' comparison are in the online Supplementary Information (Items S1 and S2).

2.2. Field methods

To investigate the stratigraphic structure of the shallow island sediments, a coarse survey was conducted on Pintail Island using a cone penetrologger (Eijkelkamp, Giesbeek, The Netherlands). This device measures instantaneous resistance to penetration in a 1D profile of 80 cm depth, which is related to grain size distribution (Stark et al., 2012). The island was surveyed at 15 points near each of the 9 groundwater monitoring locations described below. At each point, five replicate penetrologger trials were performed. The penetrologger was pushed at a constant speed of 2 cm/s. The instrument cone diameter was 5 cm. Undisturbed sediment samples were also collected at 20 cm and 70 cm depths at a location near well pair L1 and analyzed using a Hyprop and associated software (Decagon Devices, Inc., Pullman, WA) to produce example soil water retention curves and hydraulic properties including saturated hydraulic conductivity.

To measure environmental factors at the island, a micrometeorological station (Onset HOBO, Bourne, MA) was installed near well pair N2. It was placed away from trees at a horizontal distance roughly three times the height of the tallest nearby willows. The weather station recorded precipitation, wind speed, wind direction, shortwave and photosynthetically active solar radiation fluxes, humidity, air temperature, and atmospheric pressure every 5 min at 3 m above ground surface.

The groundwater table and surrounding surface water levels were monitored over time by a network of piezometers and data loggers. Piezometer pairs were installed in four general transects (N, M, L, DL, Fig. 1), and each pair included a shallow and a deep piezometer. For convenience, these short-screened and vertically nested piezometers are referred to as 'wells' in this study. The method of installation was as follows: first, a penetrometer survey was conducted to estimate a local sediment profile. The sediment survey determined the 'shallow' and 'deep' locations of interest based on preliminary observations suggesting a two-layer system. The shallow well was targeted at a depth with a high resistance to penetration, generally 40–60 cm deep, and the deep well was

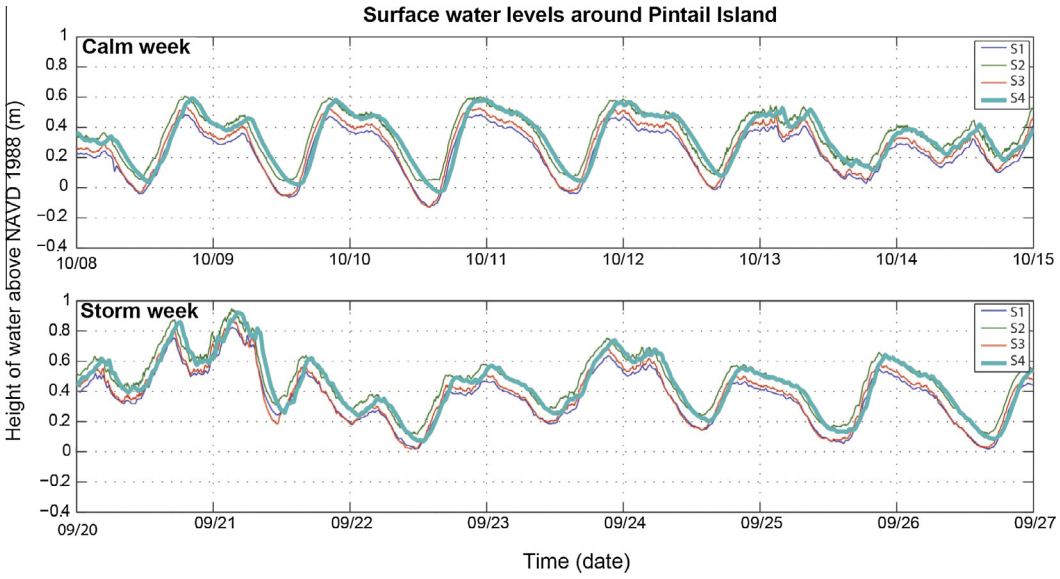

Fig. 3. Surface water heads recorded for two sample weeks: (top) the calm week of 8-October to 15-October-2013 and (bottom) the stormy week of 20-September to 27-September-2013, with storm events occurring on 20/21-September and 23/24-September. The lagoon record (S4) is in bold and green, showing the slight lag between the lagoon water level and the channel water level (S1, S2, and S3). The full 5-month time series are provided in the online Supplement. (For interpretation of the references to color in this figure legend, the reader is referred to the web version of this article.)

targeted at a depth with a low resistance to penetration, generally 80–100 cm deep. These depths were chosen to capture the groundwater conditions within two different sediment zones, as a change in the resistance to penetration reflected a change in sediment properties (i.e., grain size). For each well, a hole was augured to the depth of interest and a well, composed of a 5 cm-diameter PVC pipe attached to an 18 cm-long well screen, was installed with coarse sand around the screen. The annulus was backfilled with native silty clay. Well casings were extended above ground level to prevent flooding of the wells and loosely capped. A pressure transducer (In Situ Level Troll 300, In Situ, Inc., Ft. Collins, CO) was deployed at the bottom of each well. For surface water monitoring stations, an identical pressure transducer was attached to a fencepost driven into the river bottom such that the bottom of the logger was just touching the sediment surface. To compensate for the unvented nature of these transducers, a barometric pressure logger (BaroTroll, In Situ, Inc., Ft. Collins, CO) was installed at the island apex about 2 m above the ground on a large tree. Barometric pressure fluctuations were removed from the surface and groundwater logger data via the automated associated software (Win-Situ v.5, In Situ, Inc., Ft. Collins, CO). The accuracy of a given logger was± 1.1 cm with resolution 0.1 cm or better (In Situ, Inc., Ft. Collins, CO).

Absolute groundwater head elevations were calculated as the sum of the measured pressure head and an elevation head. The elevation head was the local ground surface elevation, determined at each well location from a Lidar dataset (NCALM, 2009), minus the measured depth to the inlet of the pressure logger. Ground surface elevation at each well cluster was taken to be the average of the nine Lidar grid cells directly surrounding the well pair. Lidar uncertainty was ±5.5 cm. Three survey campaigns attempted to further constrain elevations on the island but the easily-compactable sediment caused complications and led to data less reliable than the Lidar. Depth-to-water in each well was manually verified during the field campaigns using an e-line (Model 101 Water Level Meter, Solinst, Georgetown, ON). Well pair locations were mapped by GPS (Garmin Oregon 650T, Schaffhausen, Switzerland).

2.3. Data analysis

Water levels and environmental variables were compared using correlation and frequency analyses. Linear regressions were performed, first, to determine the correlation between surface water fluctuations and the environmental factors that might cause such fluctuations (precipitation, wind speed, river discharge, and tides), and second, to determine the correlation between a groundwater head signal and the surface water signal nearest to it. Fast Fourier transforms (FFT; Oppenheim and Schafer, 2009) were performed using the 'fft' function in MATLAB (version R2012b, Mathworks, Natick, MA) to convert all time series data to frequency data (as by Hiatt et al., 2014). Frequencies were then converted to periods so that dominant periods of dynamic response within each dataset could be identified. FFTs identified the frequencies that yielded the most significant periodicity within each time series. The FFTs of each dataset were then compared to identify similarities in periodicity among signals, which helped determine how significantly tides, wind, precipitation, and river discharge contributed to the surface water dynamics observed. Similar frequency analysis was repeated to determine how the surface water signal contributed to the observed groundwater dynamics.

Preliminary inspection of the collected datasets suggested a strong difference in system response between storm events and non-stormy time periods. To analyze this difference the study period was segmented on a daily basis using wind and rain thresholds. A day was considered 'storm-dominated' if it experienced sustained winds above 5 m/s or more than 5 mm of rain accumulation. These thresholds were chosen based on the observation that such events caused a significant disruption in the surface water patterns. Using these thresholds, the storm data subset covered 28 days, with daily average (±std. dev.) wind speed of 1.50 ± 1.38 m/s and average precipitation of 5.17 mm/day. The calm data subset covered 85 days, with average wind speed of 1.12 ± 1.21 m/s and average precipitation of 1.41 mm/day. The correlation and regression analyses were then performed for three different presentations of data: the entire study period, which extended from 9-September-2013 to 4-February-2014,

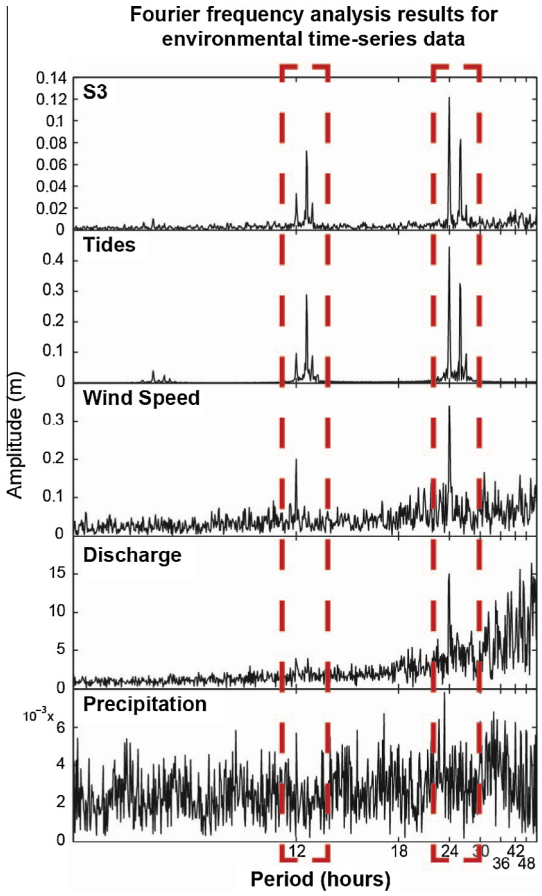

Fig. 4. Fourier frequency analysis results, expressed as recurrence period in hours, for the entire study period (9-September-2013 to 4-February-2014). Variables analyzed were: S3, the channel surface water signal (1st row), offshore NOAA tide prediction (2nd row), wind speed on Pintail Island (3rd row), Atchafalaya River discharge at Simmesport (4th row), and precipitation on Pintail Island (5th row). *Y*-axes display the amplitude of a frequency occurring at the corresponding period. The *x*-axis extent does not cover the full range of periods present in the data: it is limited to 6–48 h to highlight the most meaningful periods. Dominant periods at 12, 12.5, 24, and 25.8 h are highlighted with dashed boxes.

concatenated storm-dominated days, and concatenated non-storm-dominated days. Representative excerpts from the field data are presented herein for clarity, but the surface water, groundwater, and weather time series for the full study period are illustrated in the online Supplement.

3. Results

3.1. Surface water dynamics

Surface water levels at the monitored locations showed substantial periodicity during both calm and stormy time periods. During calm periods, surface water patterns exhibited a prominent diurnal periodicity, although in many days of the calm data set, a large peak was followed by a smaller (~5 cm) peak roughly six hours later (Fig. 3). Among the loggers located in the main channel adjacent to Pintail Island (S1, S2, and S3 in Fig. 3), the periodicity coincided in time and the signals showed no noticeable lag. For these reasons, we refer to these signals collectively as the "channel signal" and represent it by the records from S3 in the remainder of the analysis.

Lagoon water levels, represented by well S4, were slightly disconnected from channel water levels. The water level signal at S4, which was installed in the island's central lagoon, lagged one hour behind the channel signal. Storm events disturbed this lag, as well as regular diurnal/semi-diurnal periodicity. They also raised the surface water levels overall.

Linear regressions produced significant correlations ($p < 0.001$) between surface water levels and the NOAA tide prediction and between surface water levels and wind speed (Table S1). There was no significant correlation between surface water levels and river discharge (which continually increased over the study period to a peak in January and then fell, Figure S3 in Supplement), nor between surface water levels and precipitation.

Fourier analysis of the entire time series showed the channel surface water signal to be dominated by periods of 12.0, 12.5, 24.0, and 25.8 h (S3 in Fig. 4). The amplitudes of these periods, 0.03, 0.07, 0.12, and 0.08 m, respectively, add up to 0.30 m, which approximately equals the amplitude of average periodicity of surface water in the channel. To determine potential sources of these periodicities, the same analysis was performed for key environmental influences on surface water: offshore tide prediction at Point Cheveruil, discharge from the Atchafalaya River at Simmesport, and wind speed and rainfall measured by the Pintail Island weather station. The tidal prediction had dominant periods of 12.0, 24.0, and 25.8 h with respective amplitudes of 0.27, 0.43, and 0.30 m. The wind speed dataset had dominant periods of 12.0 and 24.0 h with respective amplitudes of 0.20 and 0.36 m/s. Discharge had a dominant period at 24.0 h. Precipitation data had no dominant periods.

In addition to having matching frequencies, peaks in the surface water signal corresponded in time to peaks in the tide and winds. Wind speed peaked daily at approximately 12:00, while the tidal peak shifted predictably in time (Figure S4). Surface water peaks aligned best with tidal peaks across the entire study period; however, the magnitude of each surface water peak depended on the phase difference between the tidal signal and the wind signal, with the largest surface water peaks arising from constructive interference and the smallest, most diffuse peaks influenced by destructive interference (Figure S4).

3.2. Pintail Island hydrogeologic structure

Pintail Island consists of two major hydrogeologic regions, which we roughly classify as the 'northern' region and the 'southern' region (Fig. 5). The southern region was relatively homogeneous and coarser-grained, while the northern region was finer-grained nearer to the surface (Smith, 2014). Sediment hydraulic analysis performed using the Hyprop (Decagon Devices Inc., Pullman, WA) showed that shallow (0–20 cm) sediments from the northern region were roughly an order of magnitude less hydraulically conductive than shallow (0–20 cm) sediments from the southern region (0.2 cm/day versus 1 cm/day, respectively).

A cut bank was observed on both the channel and lagoon shorelines of the more northern portions of the island, which appeared to separate the shallow, fine surficial sediments and the deeper, coarser sediments. To create a map differentiating the two hydrogeologic regions (Fig. 5), it was assumed that the northern region covered island elevations 0.45 m or more above NAVD88 (NCALM, 2009)), which was roughly the lowest elevation of the cut bank. The southern region was then assumed to cover the remainder of lower-elevation exposed land (<0.45 m elevation above NAVD88). A majority of the wells sampled the more hydrogeologically complex, layered northern region (Table 1).

3.3. Groundwater dynamics

3.3.1. Groundwater periodicity and relation to surface water dynamics

The five-month observation period captured periodic groundwater behavior that was only partially responsive to diurnal

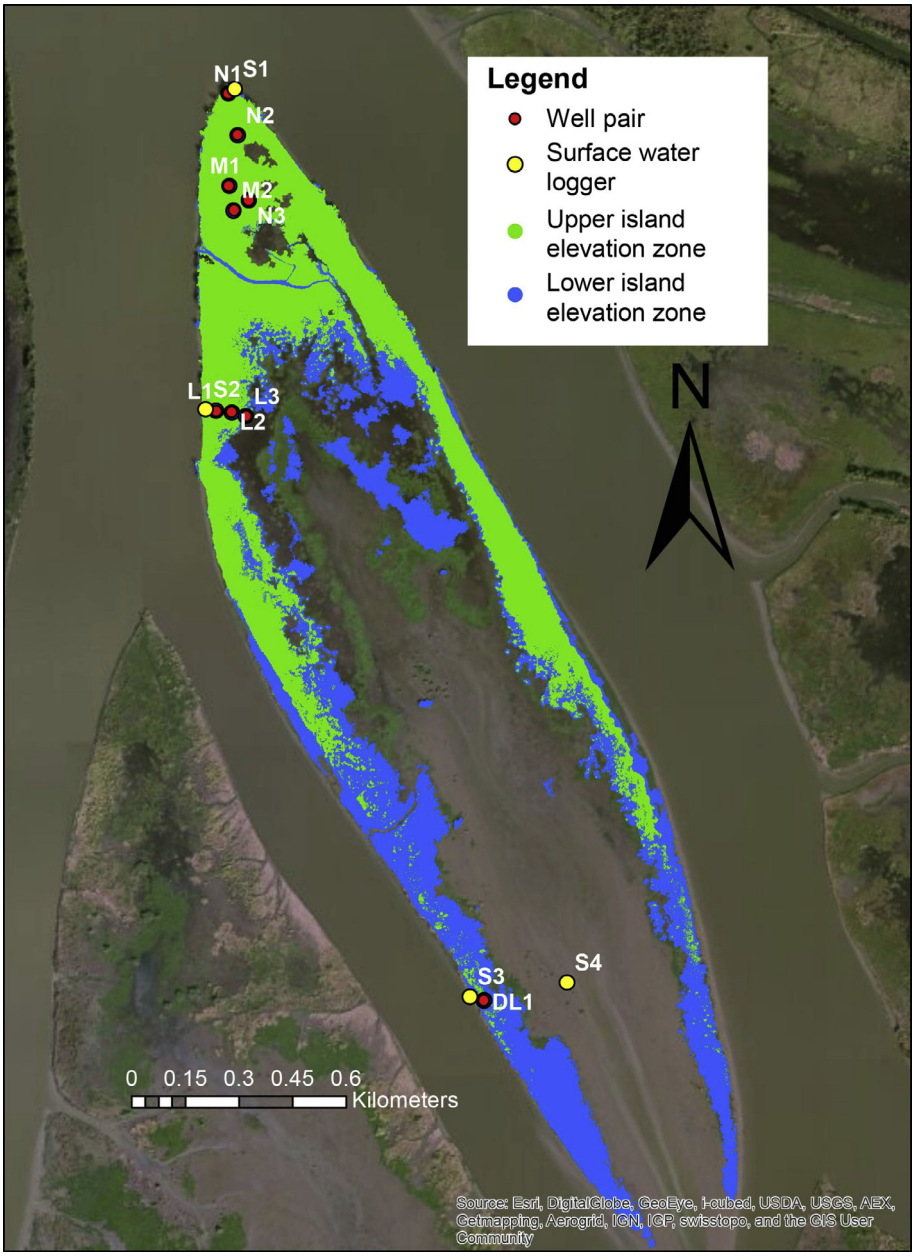

Fig. 5. Conceptual map of the shallow sedimentology of Pintail Island as determined from the penetrologger analysis and field observation. The higher-elevation, northern island zone (green) generally consists of sands overlain by finer-grained sediments. The lower-elevation, southern island zone is sandbar-like (blue). The central island lagoon/mudflat and the surrounding channels and islands are left unshaded. Background imagery from ESRI. (For interpretation of the references to color in this figure legend, the reader is referred to the web version of this article.)

surface water fluctuations and was randomly disturbed by storm events. Most wells responded to tidal surface water influence, but to varying degrees depending on their distance from the shoreline (Fig. 6). The shallow and deep wells within each well pair yielded nearly identical signals (Table 2), except in the case of pair L2, which likely had a clogged deep well. During non-stormy (calm) times, groundwater dynamics were better correlated with surface water dynamics for wells near the island edge than the island interior, especially in the higher-permeability sediments around the deep wells of N1, L1, L3, and DL1; the signals were damped and lagged, however (Table 1). Well L3-deep tracked surface water levels extremely well (r^2 = 0.98 with lagoon logger S4), and was often inundated, as it fell below the lower-permeability escarpment. Inland sites N2, N3, M1, and M2 failed to exhibit such noticeable fluctuations on the diurnal timescale of the surface water (Fig. 6, Table 3). In these inland locations the groundwater potential steadily declined over time between storm events (Fig. 6a and b).

Fourier analysis further confirmed the correlation results. All groundwater sites exhibited small but noticeable periodicity at 24.0 and 25.8 h. Wells L1, L2, L3, DL1 showed periods of 12 and 12.5 h as well (Fig. 7). At the more inland wells (N2, N3, M1, M2) the 12.0 and 12.5 h periods were absent and the 24.0 and 25.8 h period amplitudes were diminished. Overall the amplitudes of these periodic components of the groundwater signals were small. Even at sites with the strongest periodicity (L3, DL1), the dominant periods (12.0, 12.5, 24.0, and 25.8 h) together represented less than 0.06 m of amplitude (a.k.a. fluctuating groundwater head).

Table 1
Summary of the hydrogeologic zone, lag from diurnal (non-storm) surface water signal, and hydrogeologic position of each well pair in the study.

Well pair	Island hydrogeologic zone	Prominent vertical gradient	Average lag from S3, shallow well	Average lag from S3, deep well	Likely subsurface location, shallow well	Likely subsurface location, deep well
N1	High-elev., two-layer	Up	8 h 02 m	10 h 30 m	Silty clay layer	Deep silty sands
N2	High-elev., two-layer	Down	n/a[a]	n/a[a]	Transition zone between clay and sand	Deep silty sand
N3	High-elev., two-layer	None	n/a[a]	n/a[a]	Transition zone between clay and sand	Deep silty sand
M1	High-elev., two-layer	None	n/a[a]	n/a[a]	Transition zone between clay and sand	Deep silty sand
M2	High-elev., two-layer	None	n/a[a]	n/a[a]	Transition zone between clay and sand	Deep silty sand
L1	High-elev., two-layer	Up	4 h 09 m	6 h 22 m	Silty clay confining layer	Deep silty sands
L2	High-elev., two-layer	None (deep well clogged)	4 h 51 m	None (deep well clogged)	Transition zone between clay and sand	Deep silty sand
L3	Low-elev., homogeneous	Down	7 h 36 m	4 h 59 m	Lagoon silty sand	Deep silty sand
DL1	Low-elev., homogeneous	Down	1 h 44 m	3 h 01 m	Exposed silty sand	Deep silty sand

[a] These locations did not reflect diurnal surface water dynamics and so a lag duration could not be calculated.

3.3.2. Groundwater response to calm vs. stormy time periods

As in the surface water, the groundwater exhibited distinct hydrologic behavior between stormy and non-stormy days. During stormy days, groundwater tended to strongly mimic the behavior of the surrounding surface water, mostly independent of spatial location (Fig. 6, Table 3). Within these relatively brief (1–2 day) stormy periods, the groundwater levels peaked at maximum total head values similar to the nearby surface water stage. The groundwater peaks during storm events lagged behind the surface water peaks, although the lag was less during storms than it was during calm times.

For two storms in particular, on 20 September 2013 and 21 October 2013, groundwater potentials rose extremely quickly and nearly uniformly across the island, except for at the highest elevation well, N1, indicating flooding of most of the island. Also, the double-peaked tidal behavior observed during calm conditions disappeared from both the surface water and groundwater signals during storms. Following each storm event was a transition period: for inner-island sites, the groundwater potentials steadily declined over time between storms; for island-edge sites, groundwater potentials also declined but also regained surface water-like periodicity (Fig. 6). An analysis of the rate of rise and fall observed in the wells is included in the Supplement.

3.3.3. Horizontal groundwater gradients

Depending on the location within the island and the nearby surface water stage, groundwater gradients could be directed either into or out of the island, or could oscillate. In the interior of the high-elevation, northern section of the island, flow was typically outward from location N2, past N1 toward the delta channel (N2 > N1, Fig. 6b; N2–N1 positive, Fig. 8b). However, flow was often inward from the channel to the bank (S1 often > N1, Fig. 6b; N1–S1 often negative, Fig. 8b), except for the few hours during high tide when the direction was reversed (i.e., outward from N1 to S1). Reverse flow in this portion of the island bank was also observed following flooding storm events, which raised the groundwater level around N1, driving flow inward from N1 toward N2 and outward from N1 toward S1 (Fig. 6a; Fig. 8a). On the other side of the island apex, near the central island lagoon, flow was again typically outward from N2, toward N3 and the lagoon (N2 > N3, Fig. 6b; N3–N2 negative, Fig. 8b).

Wells located within the mid-island (L) transect behaved similarly to those in the apex (N) transect. Heads generally directed flow outwards from the center of the transect (L2). The overarching direction of flow across the transect was typically toward the lagoon (L1 ≈ L2 > L3, Fig. 6c and d; L3–L2 negative, Fig. 8c and d). The near-lagoon flow direction temporarily reversed from L3 toward L2 (Fig 6c) on rare occasions, during large storm recessions. In contrast, the gradient between the surface water (S2) and the location nearest the channel (L1) regularly reversed direction with the tides. Most of the time flow was inward from the channel (S2 > L1, Fig. 6d; L1–S2 negative, Fig. 8d), except for a few hours during low tide when the direction was reversed (i.e., outward from L1 to S2).

At the lowest-elevation, most bayward location, in the southern, sandbar-like zone of the island (DL1), gradients also oscillated but on a more predictable diurnal timescale. During high surface water levels, flow was inward from the channel (S3 > DL1, Fig. 6e and f and DL1–S3 negative, Fig. 8e and f) and there was zero gradient between the sandbar and the lagoon (S4–DL1 ≈ 0, Fig. 8e and f). During low surface water levels, flow was outward from the sandbar toward both the channel (DL1 > S3, Fig. 6e and f and DL1–S3 positive, Fig. 8e and f) and the lagoon (S4–DL1 negative, Fig. 8e and f). Storms perturbed the periodicity but did not eliminate the overall pattern or sense of the oscillations. However, whether during stormy or calm times, the channel water level was consistently slightly higher than the lagoon water level (S4–S3 negative, Fig. 8e and f). This difference in head led to a predominant overarching flow direction; flow was directed through the sandbar, from the channel to the lagoon.

3.3.4. Vertical groundwater gradients

Throughout the island, the shallow and deep wells within a pairing behaved very similarly (Table 2) and were typically in vertical hydrostatic equilibrium, with vertical heads agreeing within the relative uncertainty of the difference between two logger measurements (0.022 m, Fig. 9). Some apparent differences were due to well clogging (in N3-shallow after 4-November-2013 and in L2-deep); these data were omitted from most analyses but were included in the correlations of Table 2. The area in the central portion of the island apex around N2 appeared to consistently act as a recharge zone with downward flow. Larger storm events (e.g., on 5-October in Fig. 9) flooded the island, establishing surface water as a major source for this recharge. The vertical gradient at the island apex (N1) showed some indication of upward flow, representing a corresponding discharge zone. During flooding storm events, however, the gradient at N1 was reduced to vertical hydrostatic equilibrium or perhaps even temporary downward flow (if the reduced gradient was still accurate, though it fell within the uncertainty of the measurements). The vertical gradient at the

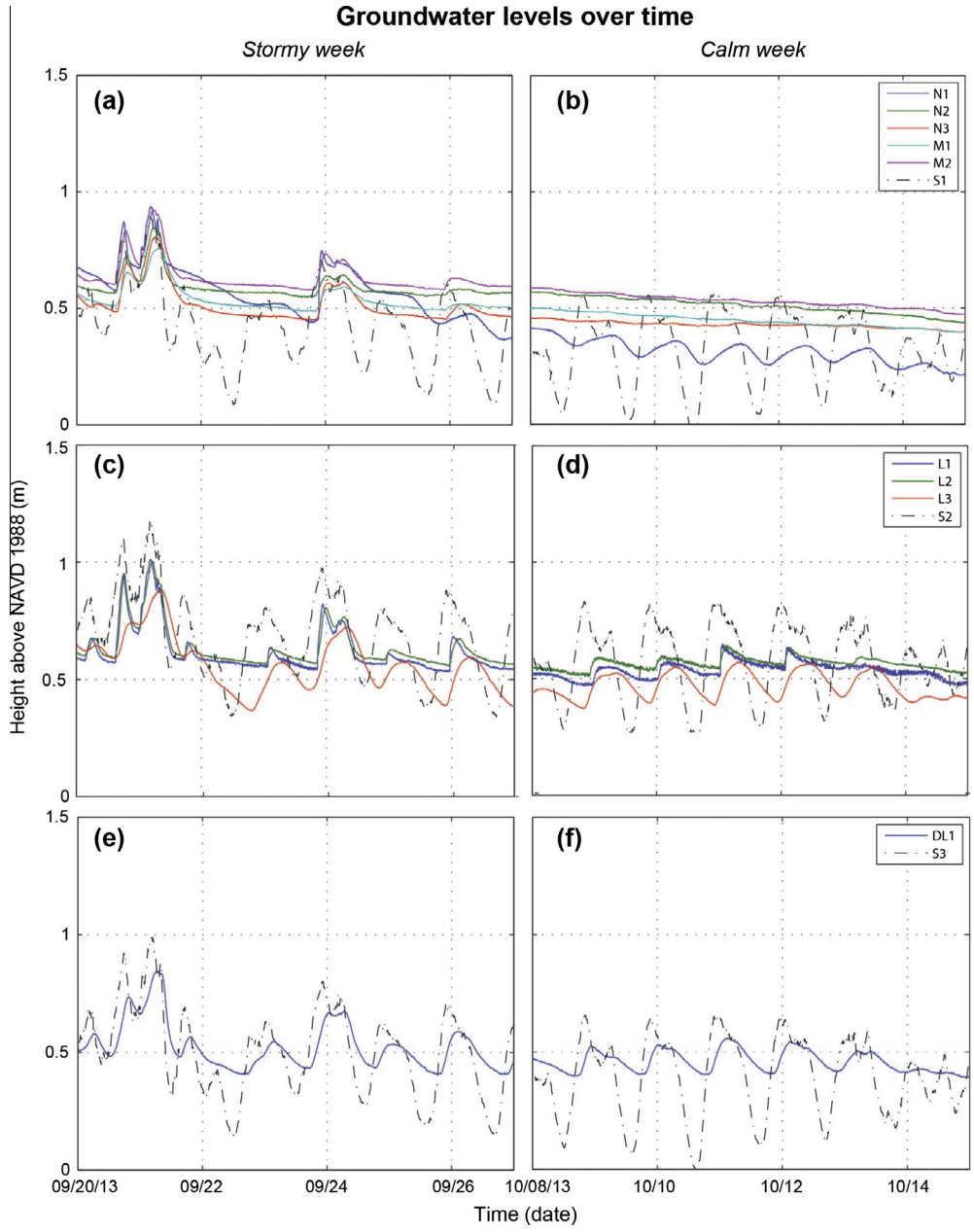

Fig. 6. Total heads from the deep wells (except L2, which displays the shallow well data) and the nearest surface water logger. (a, c, e) A stormy week between 20-September and 27-September-2013, with storm events occurring on 20/21-September and 23/24-September. (b, d, f) A calm week between 8-October and 15-October-2013. The full 5-month time series are provided in the online Supplement.

Table 2
Correlation coefficients (r^2) between the shallow and deep wells at each paired well location. Significance is $p < 0.001$ for all calculations. The unusually low correlation at L2 is likely explained by clogging in the deep well.

Cluster	N1	N2	N3	M1	M2	L1	L2	L3	DL1
Correlation	0.89	0.86	0.75	0.93	0.99	0.97	0.65	0.98	0.94

most bayward and low-elevation island site, DL1, indicated consistent downward flow (recharge) that was maintained throughout the tidal cycle and maintained, though reduced, during storm events (Fig. 9, DL1). Fig. 9 again highlights the difference in groundwater dynamics between the interior of the island apex (left column) and the island edge near the main delta channel (right column). As noted previously (see Fig. 6 and Section 3.3.3), interior island sites exhibited periodic behavior mainly when perturbed by a storm event, whereas island edge sites showed daily periodicity.

4. Discussion

4.1. Delta island hydrologic dynamics

The surface water hydrology surrounding Pintail Island during the study period (9-September-2013 to 4-February-2014) was dominated by diurnal and semi-diurnal tidal signals and semi-diurnal wind signals that caused water level fluctuations ranging from 20 cm to over 1 m. Small changes in surface water levels greatly affected island inundation patterns, as the entire relief of the island was only about 50 cm. Visual inspection of the data showed that the surface water maxima did regularly correspond in time with the wind speed maxima and tidal maxima in addition to having

Table 3
Correlation coefficients (r^2) between groundwater signals and the nearest surface water signal, separated for the storm data set and calm data subsets. Significance is $p < 0.001$ for all calculations. L2-deep omitted due to well clogging.

Shallow wells	N1	N2	N3	M1	M2	L1	L2	L3	DL1
Correlation – calm data set	0.19	0.09	0.23	0.19	0.11	0.52	0.60	0.51	0.53
Correlation – storm data set	0.35	0.36	0.35	0.49	0.46	0.66	0.84	0.71	0.77
Deep wells									
Correlation – calm data set	0.25	0.06	0.20	0.07	0.12	0.61		0.98	0.61
Correlation – storm data set	0.32	0.26	0.43	0.32	0.44	0.80		0.98	0.76

matching frequencies (see Supplement). The modest amplitudes of the peaks in the surface water signal at these wind- and tide-induced frequencies (Fig. 4) were due to the phase difference between these two signals creating alternating constructive and destructive interference (Figure S4). Although other Earth processes could influence the system on diurnal and semi-diurnal timescales, our focus on wind and tidal processes is consistent with rational conceptualization of this coastal delta system and with prior studies. For example, Kineke, Allison, and others previously identified the importance of cold fronts and onshore winds on suspended sediment deposition in such near-shore marine environments (Roberts et al., 1989; Allison et al., 2000; Kineke et al., 2006). Geleynse et al. (2014) and Hiatt et al. (2014) also identified wind as a dominant factor in surface water level fluctuations in the Wax Lake Delta.

Surprisingly, frequency analysis showed that river discharge contributed little to the groundwater response within Pintail Island during the 5-month study period. While this study was conducted during the season of typically low discharge (September to February), it did include a prolonged period of elevated discharge comparable to values observed during the higher-discharge spring season. Discharge above 5000 m^3/s was recorded at Simmesport for approximately 45 days (19 December 2013 to 02 February 2014; Figure S3) while delta surface water levels remained relatively unchanged (Figure S7). It is possible that a study conducted during the high-discharge spring season would yield different results, but evidence for that is not seen in this work. There is other evidence, however, of more extreme runoff events affecting surface water elevation at WLD. Landsat imagery shows that extreme flood and storm events can provide enough water to inundate nearly the entire delta (Geleynse et al., 2014; Smith, 2014), even at elevations above those locations found to be flooded during this study, and that these extreme flood events are closely tied to sediment deposition (Wellner et al., 2005). Together, these findings suggest that extreme events will influence delta surface water levels but smaller, although still elevated, discharge events will not; the threshold between these two behaviors cannot yet be determined from the available analysis, however.

Surface water was heavily influenced by storm events during the study, which brought high winds and heavy rains but left the tide unaltered. During storms, the regular semi-diurnal tidal signal was overwhelmed by larger surface water fluctuations, likely predominately from winds (Kineke et al., 2006; Geleynse et al., 2014). This was also reflected in the groundwater: storms induced single, diffuse peaks in the groundwater heads corresponding to the time of the storm and temporarily eliminated the double (semi-diurnal) tidal peaks (Fig. 6 and S4). During the study period, storm occurrence appeared temporally random, with no dominant recurrence

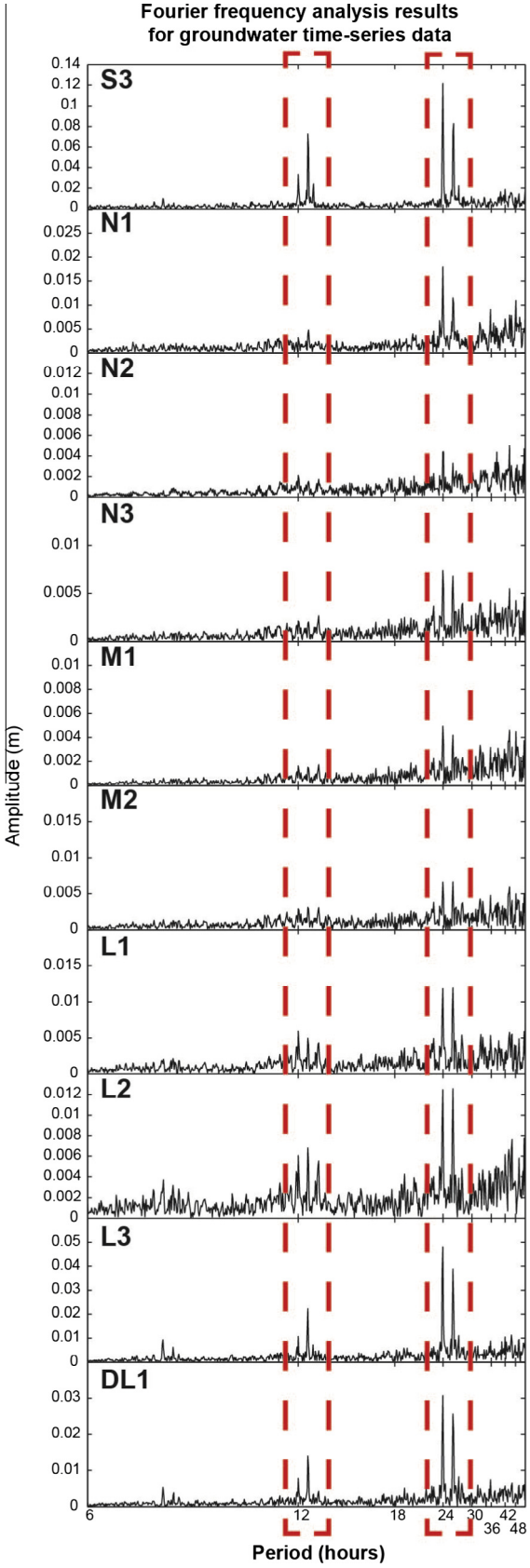

Fig. 7. Fourier frequency analysis results for surface water data (S3) and groundwater wells for the entire study period (9-September-2013 to 4-February-2014). All data are from deep wells except L2, which is from the shallow well. The dashed boxes correspond to the dominant periods (12, 12.5, 24, and 25.8 h) of surface water.

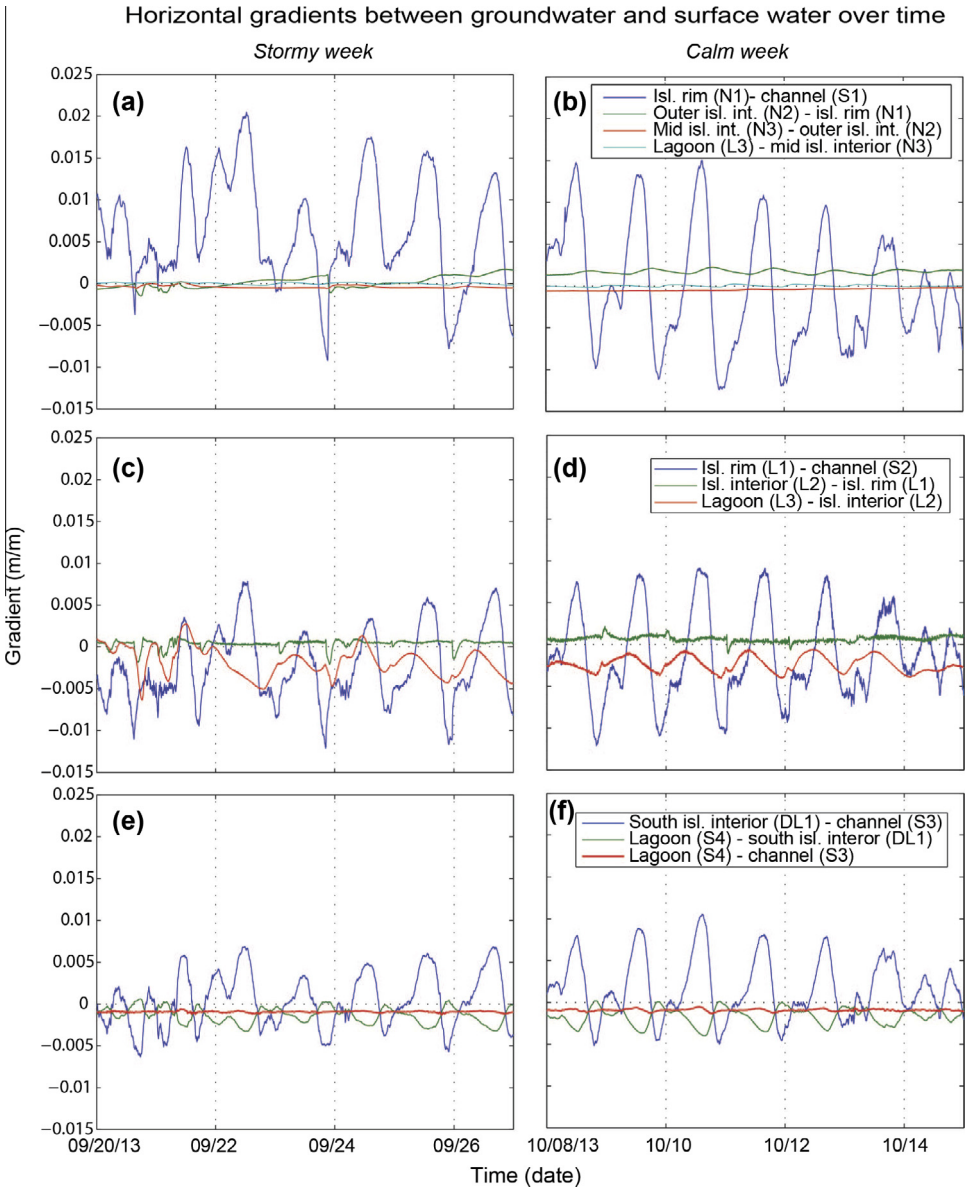

Fig. 8. Horizontal gradients between neighboring wells and surface water in each transect. All data are from deep wells except L2, which is from the shallow well. (left column) Stormy week between 20-September and 27-September-2013, with storm events occurring on 20/21-September and 23/24-September. (right column) Calm week between 8-October and 15-October-2013.

frequency. However, Allison et al. (2000) showed that wintertime cold fronts in Atchafalaya Bay may occur periodically on a three to ten day interval. It is likely that our study period was too short to capture such lower-frequency patterns.

This study also identified a lag between the lagoon surface water signal (S4), measured at the bayward mouth of the lagoon, and the signal at the apex of the lagoon, measured by well pair L3. This lag was typically between 4 and 6.5 h, but is likely exaggerated due to the location of the well logging that data. Well L3 measured a groundwater signal for a site that was often, but not always inundated across the duration of the study. Therefore, its signal likely represents an exaggerated lag in comparison to surface water, especially during times when it was not directly inundated. Despite this, the presence of a lagoon surface water lag identified here is consistent with the lagoon surface water transport patterns and timescale determined by Hiatt et al. (2014). This lag is significant for this study in that it induced oscillating gradients across the island groundwater system that were not previously identified.

4.2. Hydrogeologic heterogeneity and groundwater flow

Pintail Island hydrogeology was elevation-dependent, suggesting that different islands and portions of islands throughout a young, prograding coastal delta serve different hydrological and biogeochemical functions. The subaerial elevation distribution of Pintail Island appeared to be bimodal (NCALM, 2009; Smith, 2014). Higher island elevations hosted a bi-layer system of fine sediments over coarser (Smith, 2014), causing more damped groundwater dynamics. Lower elevations were largely homogeneous sandy sediments with strongly diurnal wind and tide-influenced groundwater dynamics. A representation of the groundwater flow regimes found in this study is presented in a conceptual model (Fig. 10).

Groundwater signals within islands are often a damped reflection of surrounding surface water signals, with the amount of damping depending on the distance of the signal from the surface water boundary and the permeability of the intervening porous medium (Li and Barry, 2000). Consistent with this, groundwater

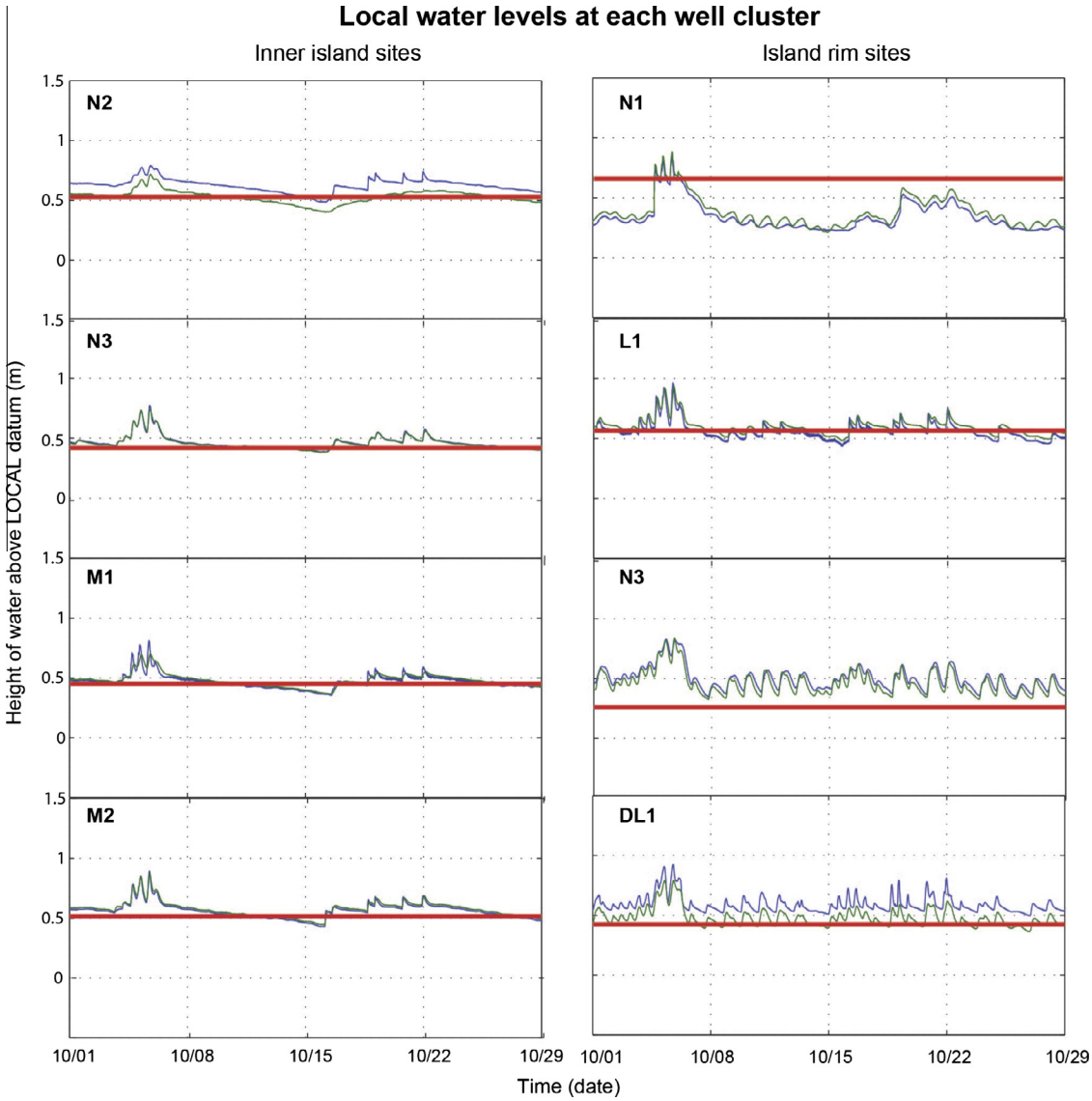

Fig. 9. Water levels in shallow (blue) and deep (green) wells for October 2013. The vertical datum is NAVD 88. The red line in each plot represents the local ground surface elevation. (left column) Interior island sites. Notable peaks are due to storm events. (right column) Island-edge sites. Differences less than 0.11 m are within the elevation uncertainty. (For interpretation of the references to color in this figure legend, the reader is referred to the web version of this article.)

at near-shore well locations among higher island elevations was somewhat influenced by tides and diurnal winds but more inland locations were not. Inland locations, rather, were only intermittently disturbed by storms, especially large, flooding storms, which occur only rarely (Smith, 2014). The rapid rise of inland groundwater heads during large storms, matching surface water rise, is best explained by the mechanical loading of the flood waters (van der Kamp and Maathuis, 1991) since gradients were small and so flow must be very slow through these low-conductivity media (K_s from 0.2 to 1 cm/day). These storm moments were the only observed occasions for recharge in the interior of the island apex, suggesting that the dominant groundwater driver in this zone is storm events.

Following flooding, the inland groundwater heads of this northern zone exhibited a prolonged recession that gradually dissipated the pressure mound created by storm recharge. Dissipation occurred at a relatively constant rate of ~3 cm head loss per day between storm events (slight slope of N2, N3, M1, M2 lines in Fig. 6a). Groundwater flow during these calm periods was persistently directed outward from the high elevation portion of the island apex toward the channel and lagoon for days to weeks after a storm (N2 toward N1 and N3; L1 ≈ L2 toward L3, Fig. 6a and b). These flows would be very slow due to the small gradients across a low-conductivity medium, and so this northern part of the island would exhibit long groundwater residence times throughout. This gradual drainage was the predominant flow regime observed during the study in the island interior.

The groundwater in the corresponding discharge zone of the island apex, around N1, experienced a faster post-storm recession rate (~13 cm/day, Fig. 6a). N1 was located in the outer levee of the island, at the highest elevations, near the channel, and among black willow (*Salix nigra*) trees; this was also likely where the layer of fine material was thickest (40–50 cm). The proximity to shore of N1 likely allowed more rapid groundwater exchange with the channel bank, causing the steeper recession rates. It is also possible that black willow evapotranspiration helped lower the shallow groundwater potential relative to the deeper potential at this location, contributing to the observed signal. Unlike the more inland groundwater, diurnal cycling of groundwater head was observed here in the island bank, even during recession periods, and in

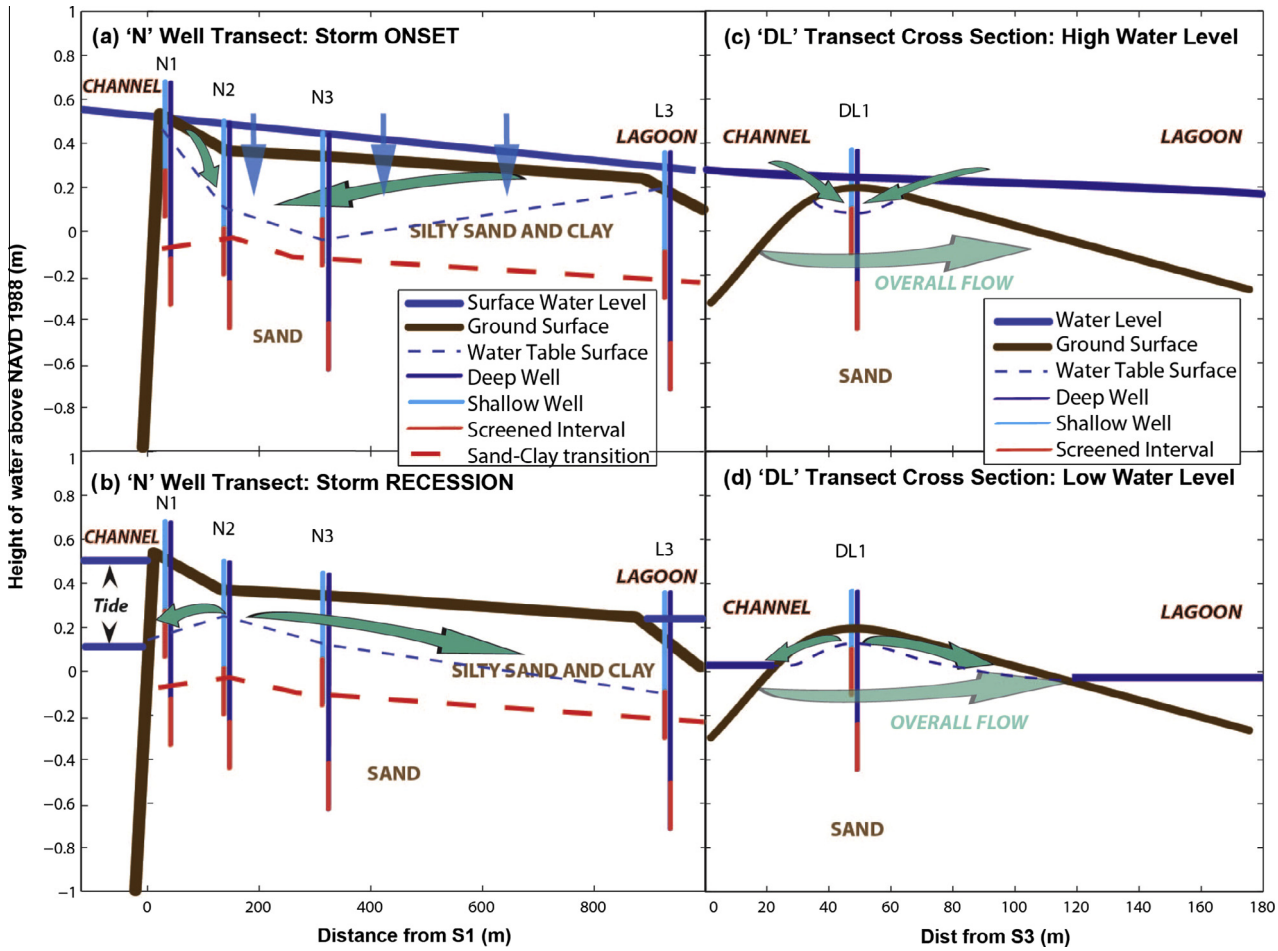

Fig. 10. Conceptual models of the differing dynamics in the two hydrogeologic regions of Pintail Island. The left column depicts the dynamics in the layered aquifer at high island elevations during periods of storm onset (top) and storm recession (bottom). The right column depicts the dynamics in the sandbar-like aquifer at low island elevations during diurnal high water (top) and diurnal low water (bottom). Models are to scale, with elevations relative to NAVD88; however, the water level representations are generalized based on data. Arrows represent predominant groundwater flow directions.

extreme cases this caused flow reversal. These reversals in groundwater gradients likely prolong the groundwater residence time within the island banks, with important biogeochemical consequences.

The biogeochemical consequences of flow reversal are likely even greater in the lower-elevation, sandbar-like zone of the island. The close correspondence between surface water and groundwater dynamics at low island elevation indicates better hydrologic connection between the groundwater and surrounding surface water through its more permeable sediments. Additionally, surface water elevations frequently exceeded ground surface here, so groundwater fluctuations were also influenced by mechanical loading (van der Kamp and Maathuis, 1991). The gradient between the sandbar (around DL1) and the channel (S3) oscillated on the tidal timescale. In contrast, the gradient between the sandbar and the lagoon (S4) was consistently either negligible or inward, towards the lagoon; flow did not appear to occur from the lagoon to the sandbar. This combination of circumstances would create a pumping effect with relatively rapid surface water/groundwater exchange. Water would enter the sandbar from the channel during high tide, be temporarily detained, and then discharge to both the channel and lagoon during low tide. Both portions of this groundwater discharge would likely be biogeochemically altered compared to the source surface water (Anschutz et al., 2009), but the latter portion would represent a net fluid transfer from channel to lagoon and a previously unidentified source of water to the lagoon. From a biogeochemical perspective, the relatively faster groundwater flow through this low elevation zone of the island (blue in Fig. 5) could allow for dissolved organic carbon concentrations to remain sufficiently high for the denitrification of nitrate-rich surface water in zones beneath the surficial oxygenated sediments (Musslewhite et al., 2003; Anschutz et al., 2009).

5. Conclusions

Pintail Island experiences variable yet predictable groundwater flow patterns. A large fraction of the island is inundated during storms, and inundation raises island groundwater heads significantly. This happens largely through mechanical loading but also through recharge. The behavior of the groundwater depends on its position, whether it is in the northern, higher-elevation, layered apex of the island or in the southern, lower-elevation, sandbar-like limbs.

Groundwater discharge occurs outwards from the central portion of the island apex at most times, dissipating prior storm pulses. Recharge here occurs during storms. Groundwater near the edge of the island drains relatively quickly and is in good hydraulic connection with the nearby surface water, reflecting damped and lagged surface water fluctuations. Flow reversal occurs regularly in the island banks, especially during high tides and storms, and this reversal can potentially prolong groundwater residence times.

The lower-elevation zone of the island is strongly influenced by the surface water surrounding it and is frequently inundated. Flow through the sandbar-like limbs of this zone of the island can experience alternating in/out pumping patterns as well as flow-through patterns directed across the bar from the channel to lagoon. Their oscillating and more rapid flow lend these lower-elevation portions of the islands particularly strong potential to serve as biogeochemical hotspots, including loci for denitrification.

As the Wax Lake Delta is a model system for dynamics and progradation of mixed-grain size coastal deltas, the conceptual model developed by this study for the island aquifer of a young prograding coastal delta may provide a starting point for investigating the hydrologic and nutrient budgets of other similar systems. This model allows for the scientific community to reasonably hypothesize the magnitudes and directions of groundwater flow dependent on location; for example, more rapid flow on tidal timescales exists in lower-elevation zones, while slower flood/drainage driven by storms predominates in higher-elevation zones. This characterization could help guide where and when biogeochemical investigations relevant to fluvial nutrient loading mitigation should be targeted and, with further study, help explain mechanisms necessary for island ecosystem survival and succession.

Acknowledgments

This research was funded by the University of Texas at Austin Jackson School of Geosciences Graduate Fellowship and other Jackson School support. We thank B. Carlson, P.E. Carlson, R. Flinker, D.W. Meyer, B. Minton, A. Hardison, B.C. Smith, L. Stevens, and R.W. Wagner for assistance in the field and N. Geleynse, M. Hiatt, D. Mohrig, and P. Passalaqua for advice and support in kind. We also thank M.B. Cardenas and M.H. Young for constructive manuscript edits.

Appendix A. Supplementary material

Supplementary data associated with this article can be found, in the online version, at http://dx.doi.org/10.1016/j.jhydrol.2015.02.017.

References

Alam, M., 1996. Subsidence of the Ganges—Brahmaputra delta of Bangladesh and associated drainage, sedimentation and salinity problems. In: Milliman, J.D., Haq, B.U. (Eds.), Sea-Level Rise and Coastal Subsidence. Springer, Netherlands, pp. 169–192.

Allison, M.A., Kineke, G.C., Gordon, E.S., Goñi, M.A., 2000. Development and reworking of a seasonal flood deposit on the inner continental shelf off the Atchafalaya River. Cont. Shelf Res. 20 (16), 2267–2294.

Anderson, W.P., Evans, D.G., 2002. Aquifer salinization from storm overwash. J. Coastal Res. 18 (3), 413–420. http://dx.doi.org/10.2307/4299090.

Anschutz, P., Smith, T., Mouret, A., Deborde, J., Bujan, S., Poirier, D., Lecroart, P., 2009. Tidal sands as biogeochemical reactors. Estuar. Coast. Shelf Sci. 84 (1), 84–90. http://dx.doi.org/10.1016/j.ecss.2009.06.015.

Bardini, L., Boano, F., Cardenas, M.B., Revelli, R., Ridolfi, L., 2012. Nutrient cycling in bedform induced hyporheic zones. Geochim. Cosmochim. Acta 84, 47–61. http://dx.doi.org/10.1016/j.gca.2012.01.025.

Bianchi, D.T.S., Allison, D.M.A., Cai, P.W.-J. (Eds.), 2013. Biogeochemical Dynamics at Major River-Coastal Interfaces: Linkages with Global Change. Cambridge University Press, New York, NY.

Boaga, J., D'Alpaos, A., Cassiani, G., Marani, M., Putti, M., 2014. Plant-soil interactions in salt marsh environments: experimental evidence from electrical resistivity tomography in the Venice Lagoon. Geophys. Res. Lett. 41 (17). http://dx.doi.org/10.1002/2014GL060983, 2014GL060983.

Branhoff, B., 2012. Nitrogen Biogeochemistry in a Restored Mississippi River Delta: A Modeling Approach. Louisiana State University Department of Oceanography and Coastal Sciences, Baton Rouge, LA.

Cardenas, M.B., 2010. Lessons from and assessment of Boussinesq aquifer modeling of a large fluvial island in a dam-regulated river. Adv. Water Resour. 33 (11), 1359–1366. http://dx.doi.org/10.1016/j.advwatres.2010.03.015.

Cardenas, M.B., Jiang, H., 2011. Wave-driven porewater and solute circulation through rippled elastic sediment under highly transient forcing. Limnol. Oceanogr.: Fluids Environ. 1, 23–37. http://dx.doi.org/10.1215/21573698-1151658.

Carle, M.V., Sasser, C.E., Roberts, H.H., 2013. Accretion and vegetation community change in the Wax Lake Delta following the historic 2011 Mississippi River Flood. J. Coastal Res. http://dx.doi.org/10.2112/JCOASTRES-D-13-00109.1.

Geleynse, N., Hiatt, M., Sangireddy, H., Passalacqua, P., 2014. Identifying Environmental Controls on the Shoreline of a Natural River Delta, (submitted for publication).

Gonneea, M.E., Mulligan, A.E., Charette, M.A., 2013. Seasonal cycles in radium and barium within a subterranean estuary: implications for groundwater derived chemical fluxes to surface waters. Geochim. Cosmochim. Acta 119, 164–177. http://dx.doi.org/10.1016/j.gca.2013.05.034.

Goolsby, D.A., Battaglin, W.A., Aulenbach, B.T., Hooper, R.P., 2000. Nitrogen flux and sources in the Mississippi River Basin. Sci. Total Environ. 248 (2–3), 75–86. http://dx.doi.org/10.1016/S0048-9697(99)00532-X.

Gumbricht, T., McCarthy, J., McCarthy, T.S., 2004. Channels, wetlands and islands in the Okavango Delta, Botswana, and their relation to hydrological and sedimentological processes. Earth Surf. Process. Landforms 29 (1), 15–29. http://dx.doi.org/10.1002/esp.1008.

Habib, E., Meselhe, E., 2006. Stage-discharge relations for low-gradient tidal streams using data-driven models. J. Hydraulic Eng. 132 (5), 482–492. http://dx.doi.org/10.1061/(ASCE)0733-9429(2006) 132:5(482).

Harvey, J.W., Germann, P.F., Odum, W.E., 1987. Geomorphological control of subsurface hydrology in the Creekbank zone of tidal marshes. Estuar. Coast. Shelf Sci. 25 (6), 677–691. http://dx.doi.org/10.1016/0272-7714(87)90015-1.

Henry, K.M., 2012. Linking Nitrogen Biogeochemistry to Different Stages of Wetland Soil Development in the Mississippi River delta, Louisiana. Chapter 5. A Conceptual Model of Biogeochemical Cycling During Delta Development in the Anthropocene. Ph.D. Dissertation. Louisiana State University, Department of Oceanography and Coastal Sciences.

Hiatt, M.R., Wagner, R. Wayne, Geleynse, Nathanial, Minton, Brandon, Passalacqua, Paola, 2014. A network-based analysis of river delta surface hydrology: an example from Wax Lake Delta.

Horn, D.P., 2002. Beach groundwater dynamics. Geomorphology 48 (1–3), 121–146. http://dx.doi.org/10.1016/S0169-555X(02)00178-2.

Hughes, C.E., Binning, P., Willgoose, G.R., 1998. Characterisation of the hydrology of an estuarine wetland. J. Hydrol. 211 (1–4), 34–49. http://dx.doi.org/10.1016/S0022-1694(98)00194-2.

Kim, W., Dai, A., Muto, T., Parker, G., 2009. Delta progradation driven by an advancing sediment source: coupled theory and experiment describing the evolution of elongated deltas. Water Resour. Res. 45 (6). http://dx.doi.org/10.1029/2008WR007382.

Kineke, G.C., Higgins, E.E., Hart, K., Velasco, D., 2006. Fine-sediment transport associated with cold-front passages on the shallow shelf, Gulf of Mexico. Cont. Shelf Res. 26 (17–18), 2073–2091. http://dx.doi.org/10.1016/j.csr.2006.07.023.

Kolker, A.S., Cable, J.E., Johannesson, K.H., Allison, M.A., Inniss, L.V., 2013. Pathways and processes associated with the transport of groundwater in deltaic systems. J. Hydrol. 498, 319–334. http://dx.doi.org/10.1016/j.jhydrol.2013.06.014.

Lenkopane, M., Werner, A.D., Lockington, D.A., Li, L., 2009. Influence of variable salinity conditions in a tidal creek on riparian groundwater flow and salinity dynamics. J. Hydrol. 375 (3–4), 536–545. http://dx.doi.org/10.1016/j.jhydrol.2009.07.004.

Li, L., Barry, D.A., 2000. Wave-induced beach groundwater flow. Adv. Water Resour. 23 (4), 325–337. http://dx.doi.org/10.1016/S0309-1708(99)00032-9.

Li, S., Wang, G., Deng, W., Hu, Y., Hu, W.-W., 2009. Influence of hydrology process on wetland landscape pattern: a case study in the Yellow River Delta. Ecol. Eng. 35 (12), 1719–1726. http://dx.doi.org/10.1016/j.ecoleng.2009.07.009.

McCarthy, T.S., 2006. Groundwater in the wetlands of the Okavango Delta, Botswana, and its contribution to the structure and function of the ecosystem. J. Hydrol. 320 (3–4), 264–282. http://dx.doi.org/10.1016/j.jhydrol.2005.07.045.

Moffett, K.B., Gorelick, S.M., McLaren, R.G., Sudicky, E.A., 2012. Salt marsh ecohydrological zonation due to heterogeneous vegetation–groundwater–surface water interactions. Water Resour. Res. 48 (2), W02516. http://dx.doi.org/10.1029/2011WR010874.

Musslewhite, C.L., McInerney, M.J., Dong, H., Onstott, T.C., Green-Blum, M., Swift, D., Macnaughton, S., White, D.C., Murray, C., Chien, Y.-J., 2003. The factors controlling microbial distribution and activity in the shallow subsurface. Geomicrobiol J. 20 (3), 245–261. http://dx.doi.org/10.1080/01490450303877.

NCALM, 2009. Lidar Dataset, Wax Lake Delta. National Center for Airborne Laser Mapping, Houston, TX.

Neill, C.F., Allison, M.A., 2005. Subaqueous deltaic formation on the Atchafalaya Shelf, Louisiana. Mar. Geol. 214 (4), 411–430. http://dx.doi.org/10.1016/j.margeo.2004.11.002.

Nichols, G., 2013. Sedimentology and Stratigraphy. John Wiley & Sons.

NOAA, 2014. Tide Predictions – Point Cheveruil 8764634 Tidal Data Daily View – NOAA Tides & Currents. <http://tidesandcurrents.noaa.gov/noaatidepredictions/NOAATidesFacade.jsp?Stationid=8764634> (accessed 18.04.14).

Oppenheim, A.V., Schafer, R.W., 2009. Discrete-Time Signal Processing, third ed. Prentice-Hall.

Parker, G., Sequeiros, O., 2006. Large scale river morphodynamics: application to the Mississippi Delta. In: Alves, E., Cardoso, A., Leal, J., Ferreira, R. (Eds.), River Flow 2006. Taylor & Francis.

Peyronnin, N., Green, M., Richards, C.P., Owens, A., Reed, D., Chamberlain, J., Groves, D.G., Rhinehart, W.K., Belhadjali, K., 2013. Louisiana's 2012 coastal master plan: overview of a science-based and publicly informed decision-making process. J. Coastal Res. 1–15. http://dx.doi.org/10.2112/SI_67_1.1.

Postma, D., Boesen, C., Kristiansen, H., Larsen, F., 1991. Nitrate reduction in an unconfined sandy aquifer: water chemistry, reduction processes, and geochemical modeling. Water Resour. Res. 27 (8), 2027–2045. http://dx.doi.org/10.1029/91WR00989.

Rabalais, N.N., Turner, R.E., JustiĆ, D., Dortch, Q., Wiseman, W.J., Gupta, B.K.S., 1996. Nutrient changes in the Mississippi River and system responses on the adjacent continental shelf. Estuaries 19 (2), 386–407. http://dx.doi.org/10.2307/1352458.

Reide Corbett, D., Dillon, K., Burnett, W., 2000. Tracing groundwater flow on a barrier island in the north-east Gulf of Mexico. Estuar. Coast. Shelf Sci. 51 (2), 227–242. http://dx.doi.org/10.1006/ecss.2000.0606.

Rivera-Monroy, V.H., Lenaker, P., Twilley, R.R., Delaune, R.D., Lindau, C.W., Nuttle, W., Habib, E., Fulweiler, R.W., Castañeda-Moya, E., 2010. Denitrification in coastal Louisiana: a spatial assessment and research needs. J. Sea Res. 63 (3–4), 157–172. http://dx.doi.org/10.1016/j.seares.2009.12.004.

Roberts, H.H., 1997. Evolution of Sedimentary Architecture and Surface Morphology: Atchafalaya and Wax Lake Deltas, Louisiana (1973–1994), vol. 47.

Roberts, H.H., Huh, O.K., Hsu, S.A., Rouse, Jr., L.J., Rickman, D.A., 1989. Winter Storm Impacts on the Chenier Plain Coast of Southwestern Louisiana, 39.

Röper, T., Kröger, K.F., Meyer, H., Sültenfuss, J., Greskowiak, J., Massmann, G., 2012. Groundwater ages, recharge conditions and hydrochemical evolution of a barrier island freshwater lens (Spiekeroog, Northern Germany). J. Hydrol. 454–455, 173–186. http://dx.doi.org/10.1016/j.jhydrol.2012.06.011.

Shaw, J.B., Mohrig, D., Whitman, S.K., 2013. The morphology and evolution of channels on the Wax Lake Delta, Louisiana, USA. J. Geophys. Res.: Earth Surface 118 (3), 1562–1584. http://dx.doi.org/10.1002/jgrf.20123.

Slingerland, R., Smith, N.D., 2004. River avulsions and their deposits. Annu. Rev. Earth Planet. Sci. 32 (1), 257–285. http://dx.doi.org/10.1146/annurev.earth.32.101802.120201.

Smith, B., 2014. The Effects of Vegetation on Island Geomorphology in the Wax Lake Delta, Louisiana. M.S. Thesis. The University of Texas at Austin, Austin, TX, May.

Snedden, G.A., Cable, J.E., Swarzenski, C., Swenson, E., 2007. Sediment discharge into a subsiding Louisiana deltaic estuary through a Mississippi River diversion. Estuar. Coast. Shelf Sci. 181–193. http://dx.doi.org/10.1016/j.ecss.2006.06.035.

Spalding, R.F., Parrott, J.D., 1994. Shallow groundwater denitrification. Sci. Total Environ. 141 (1–3), 17–25. http://dx.doi.org/10.1016/0048-9697(94)90014-0.

Stanley, D.J., 1990. Recent subsidence and northeast tilting of the Nile delta, Egypt. Mar. Geol. 94 (1–2), 147–154. http://dx.doi.org/10.1016/0025-3227(90)90108-V.

Stark, N., Coco, G., Bryan, K.R., Kopf, A., 2012. In-situ geotechnical characterization of mixed-grain-size bedforms using a dynamic penetrometer. J. Sediment. Res. 82 (7), 540–544. http://dx.doi.org/10.2110/jsr.2012.45.

Ursino, N., Silvestri, S., Marani, M., 2004. Subsurface flow and vegetation patterns in tidal environments. Water Resour. Res. 40 (5), W05115. http://dx.doi.org/10.1029/2003WR002702.

USGS, 2014. USGS Current Conditions for USGS 07381490 Atchafalaya River at Simmesport, LA. <http://waterdata.usgs.gov/nwis/uv?site_no=07381490> (accessed 18.04.14).

Van der Kamp, G., Maathuis, H., 1991. Annual fluctuations of groundwater levels as a result of loading by surface moisture. J. Hydrol. 127 (1–4), 137–152. http://dx.doi.org/10.1016/0022-1694(91)90112-U.

Venterink, H.O., Hummelink, E., Hoorn, M.W.V.D., 2003. Denitrification potential of a river floodplain during flooding with nitrate-rich water: grasslands versus reedbeds. Biogeochemistry 65 (2), 233–244. http://dx.doi.org/10.1023/A:1026098007360.

Viparelli, E., Shaw, J., Bevington, A., Meselhe, E., Holm, G., Mohrig, D., Twilley, R., Parker, G., 2011. Inundation Model As an Aid for Predicting Ecological Succession on Newly-Created Deltaic Land Associated with Mississippi River Diversions: Application to the Wax Lake Delta. In: World Environmental and Water Resources Congress 2011. American Society of Civil Engineers, pp. 2340–2349.

Wellner, R., Beaubouef, R., Van Wagoner, J., Roberts, H., Sun, T., 2005. Jet-plume depositional bodies—the primary building blocks of Wax Lake Delta. Gulf Coast Assoc. Geol. Soc. Trans. 55, 867–909.

Wilson, A.M., Moore, W.S., Joye, S.B., Anderson, J.L., Schutte, C.A., 2011. Storm-driven groundwater flow in a salt marsh. Water Resour. Res. 47 (2), W02535. http://dx.doi.org/10.1029/2010WR009496.

Zhang, H., Moffett, K.B., Windham-Myers, L., Gorelick, S., 2013. Hydrological controls on methylmercury flux from an intertidal salt marsh. AGU Fall Meeting Abstracts, -1, 03.